JOURNAL OF APPLIED PHYSICS **100**, 114105 (2006)

Enhanced dielectric properties of highly (100)-oriented $Ba(Zr,Ti)O_3$ thin films grown on $La_{0.7}Sr_{0.3}MnO_3$ bottom layer

X. G. Tang,[a] Q. X. Liu, and Y. P. Jiang
School of Physics and Optoelectric Engineering, Guangdong University of Technology, 729 East Dongfeng Road, Guangzhou 510090, People's Republic of China

R. K. Zheng and H. L. W. Chan
Department of Applied Physics, Materials Research Centre, The Hong Kong Polytechnic University, Hung Hom, Kowloon, Hong Kong, People's Republic of China

(Received 4 June 2006; accepted 10 September 2006; published online 6 December 2006)

Barium zirconate titanate $Ba(Zr_{0.2}Ti_{0.8})O_3$ (BZT) thin films on $La_{0.7}Sr_{0.3}MnO_3$ (LSMO)-coated Si and $Pt/Ti/SiO_2/Si$ substrates have been prepared by pulsed laser deposition and crystallized *in situ* at 650 °C. Four capacitor types of LSMO/BZT/LSMO/Si, Pt/BZT/LSMO/Si, Pt/BZT/Pt/Si, and Pt/BZT/LSMO/Pt/Si were prepared to investigate the structural and dielectric properties, tunability, and figure of merits. Among them, the high (100)-oriented BZT films were grown on the (100)-textured LSMO and (111)-textured Pt electrodes. The results show that the LSMO/BZT/LSMO/Si has the highest dielectric constant of 555 and Pt/BZT/LSMO/Pt/Si has the highest tunability of 73% at 1 MHz. The high dielectric constant and tunability have been attributed to the (100) texture of the LSMO bottom layer leading to the decrease of the thickness of the interface of the dead layer. © *2006 American Institute of Physics*. [DOI: 10.1063/1.2393010]

I. INTRODUCTION

Barium strontium titanate $(Ba,Sr)TiO_3$ (BST) thin films have currently become very attractive for applications in decoupling capacitors, storage capacitors, and dielectric field tunable elements for high frequency devices.[1,2] The high dielectric constant and low loss make BST one of the promising candidates for dynamic random access memory (DRAM) and tunable microwave device applications. The large electrical-field-dependent dielectric constant can be used for devices such as tunable oscillators, filters, and phase shifters. In such devices, it is desirable to have a high dielectric tunability in a certain electric field range and low dielectric loss. $Ba(Zr_yTi_{1-y})O_3$ (BZT) is a possible alternative to BST in the fabrication of ceramic capacitors because Zr^{4+} is chemically more stable than Ti^{4+}.[3–6] The nature of the ferroelectric phase transition at the Curie temperature (T_C) of BZT bulk ceramics is known to change strongly with Zr content. At higher Zr contents ($y \sim 0.20$), only one phase transition exists.[3] The fabrication of BZT thin films by pulsed laser deposition (PLD),[7] rf-magnetron sputtering,[8] and sol-gel method[9,10] and their dielectric properties have been reported recently.

Many efforts have been made to improve the dielectric properties of the BST thin film capacitors, including using conductive oxide electrodes such as $(La_{0.7}Sr_{0.3})MnO_3$,[11] $(Ba,Sr)RuO_3$,[12] $LaNiO_3$,[13] and $YBa_2Cu_3O_{7-\delta}$ (YBCO).[14] There are a few papers that reported on the effects of conductive oxide electrodes on the dielectric properties of BZT films. Zhai *et al.* reported the dielectric properties of $B(Zr_{0.35}Ti_{0.65})O_3$ thin films using $LaNiO_3$ as a buffer layer.[15] The effects of $(La_{0.7}Sr_{0.3})MnO_3$ bottom electrode on the dielectric properties and tunability of BZT films has not yet been reported. In this work, $Ba(Zr_{0.2}Ti_{0.8})O_3$ thin films grown on Si(100) and $Pt(111)/Ti/SiO_2/Si(100)$ substrates with $(La_{0.7}Sr_{0.3})MnO_3$ bottom electrode layer were prepared by a pulsed laser deposition (PLD) method. The (100)-orientation characteristics of grains, dielectric properties, tunability, and figure of merit of the BZT thin films on Si and $Pt/Ti/SiO_2/Si$ substrates with $(La_{0.7}Sr_{0.3})MnO_3$ bottom electrode layer are also reported.

II. EXPERIMENT

A. Deposition of BZT/LSMO heterostructure thin films

The $Ba(Zr_{0.2}Ti_{0.8})O_3/(La_{0.7}Sr_{0.3})MnO_3$ (BZT/LSMO) heterostructure thin films were grown on Si and $Pt/Ti/SiO_2/Si$ substrates kept at 650 °C by PLD using a KrF excimer pulsed laser ($\lambda = 248$ nm) and BZT and LSMO targets. These BZT and LSMO targets were prepared by sol-gel process[16] and conventional solid state reaction,[17] respectively. The films were deposited at a laser repetition rate of 10 Hz and pulsed laser energy of 300 mJ. The base pressure of the system is 2 mTorr. The deposition times are 30–40 min for BZT films and 10 min for LSMO electrodes. And the deposition rate was 20 nm/min. The oxygen pressure was an important parameter and was kept at 200 mTorr. Finally, the LSMO bottom electrodes were crystallized *in situ* at 650 °C in 400 mTorr of oxygen for 10 min and cooled down slowly to room temperature and polycrystalline LSMO electrodes were fabricated. Similarly, the BZT thin films were crystallized *in situ* at 650 °C in 400 mTorr of oxygen for 10 min and cooled down slowly to room temperature and preferentially (100)-oriented BZT/LSMO heterostructure thin films were fabricated. Details of the deposition conditions are given in Ref. 18 and Table I. The

[a] Author to whom correspondence should be addressed; FAX: +86-20-3932 2265; electronic mail: xgtang6@yahoo.com

 © 2006 American Institute of Physics

TABLE I. Deposition conditions of BZT thin film and LSMO electrodes by PLD.

Deposition parameters	$Ba(Zr_{0.2}Ti_{0.8})O_3$ and $(La_{0.7}Sr_{0.3})MnO_3$
Deposition method	PLD
Deposition temperature	650 °C
Film thickness	200–800 nm
Base vacuum	2×10^{-6} Torr
Energy used	300 mJ/pulse
Repetition rate	10 Hz
Deposition time	10–40 min
Working pressure	200×10^{-6} Torr
Annealing temperature	650 °C
Substrates	Si(100) and Pt/Ti/SiO_2/Si

thicknesses of the as-grown BZT and LSMO thin films were measured by a Tencor P-10 surface profiler (KLA-Tencor Corporation, USA) and were about 600–800 and 200 nm, respectively.

B. Measurement

The crystalline structure of the BZT/LSMO heterostructure thin films on Si and Pt/Ti/SiO_2/Si substrates were analyzed by a Philips PW3710 x-ray diffractometer using Cu $K\alpha$ radiation with a Ni filter. For electrical measurements of the BZT/LSMO heterostructure thin film capacitors, top platinum (Pt) and LSMO electrodes of 0.2 mm diameter were deposited through a shadow mask onto the BZT thin films by PLD. The resistivity of the LSMO film on Si substrate at room temperature measurements using a standard four-point method was $6.4\times10^{-4}\ \Omega$ cm. The four capacitor types prepared in this study were Pt/BZT/LSMO/Si, LSMO/BZT/LSMO/Si, Pt/BZT/Pt/Ti/SiO_2/Si, and Pt/BZT/LSMO/Pt/Ti/SiO_2/Si. The polarization–electric field (P-E) hysteresis loops were obtained using a TF Analyzer 2000 (aixACCT, Aachen, Germany) system; the input signal was sinusoidal with a frequency of 100 Hz. The dielectric properties and C-V characteristics of BZT/LSMO heterostructure thin film capacitors were measured by using an Agilent 4294 A impedance analyzer at room temperature. All measurements were performed as cycle sweeps (zero voltage to positive voltage back to zero voltage, zero voltage to negative voltage back to zero voltage) to check for any possible hysteretic behavior.

III. RESULTS AND DISCUSSION

A. Structure and the type of capacitors

Figure 1 shows the x-ray diffraction (XRD) patterns of the LSMO bottom electrode and BZT/LSMO heterostructure thin film on Si substrates annealed for 10 min in oxygen atmosphere at 650 C. The XRD result also exhibits that the thin films annealed at 650 °C have very strong (100) orientation. Six peaks, (100), (110), (111), (200), (210), and (211), were observed in the XRD patterns of the LSMO and BZT/LSMO thin films. The relative peak intensities of $\Sigma I(h00)/\Sigma I(hkl)$ are found to be 0.59 and 0.87, respectively, for LSMO and BZT/LSMO thin films on Si substrates, indicating a remarkably strong (100) grain orientation for LSMO

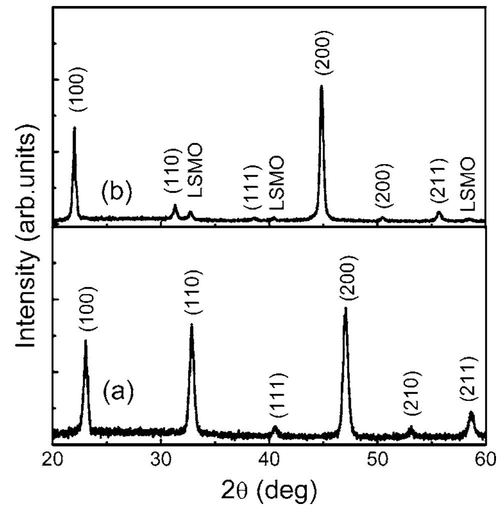

FIG. 1. X-ray diffraction patterns of LSMO and BZT thin films deposited on (a) Si and (b) LSMO/Si substrates crystallized *in situ* at 650 °C for 10 min.

and BZT/LSMO films. The high (100) orientation of BZT thin film on LSMO-coated Si substrate has been attributed to the (100) texture of the LSMO film on Si substrate.

Figure 2 shows the XRD patterns of the BZT thin film on Pt/Ti/SiO_2/Si substrates without and with a LSMO buffer layer and annealed for 10 min in oxygen atmosphere at 650 C. The XRD result also exhibits that the thin films annealed at 650 °C have very strong (100) orientation. Six peaks, (100), (110), (111), (200), (210) and (211), were observed in the XRD patterns of the BZT/LSMO thin films. The relative peak intensities of $\Sigma I(h00)/\Sigma I(hkl)$ are found to be 0.98 and 0.60, respectively, for BZT thin film on Pt/Ti/SiO_2/Si substrates without and with a LSMO buffer layer, indicating a remarkably strong (100) grain orientation. Previously we have reported that $(Pb,Ca)TiO_3$ thin films on Pt/Ti/SiO_2/Si substrate crystallized with (100) axis orientation, in accordance with minimum surface energy conditions.[19] The high (100) orientation of BZT thin films on Pt-coated Si substrate is considered to be a self-textured growth, in accordance with minimum surface energy conditions.

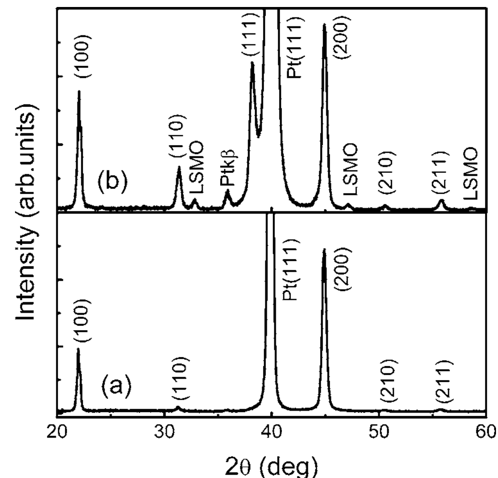

FIG. 2. X-ray diffraction patterns of BZT thin films deposited on (a) Pt/Ti/SiO_2/Si and (b) LSMO/Pt/Ti/SiO_2/Si substrates crystallized *in situ* at 650 °C for 10 min.

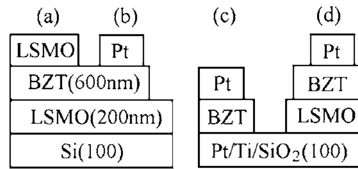

FIG. 3. Schematic illustrations of the four types of capacitors: (a) LSMO/BST/LSMO/Si, (b) Pt/BZT/LSMO/Si, (c) Pt/BST/Pt/Ti/SiO_2/Si, and (d) Pt/BST/LSMO/Pt/Ti/SiO_2/Si.

Figure 3 shows a schematic illustration of the four types of capacitors, they are LSMO/BZT/LSMO/Si, Pt/BZT/LSMO/Si, Pt/BZT/Pt/Ti/SiO_2/Si, and Pt/BZT/LSMO/Pt/Ti/SiO_2/Si, respectively.

B. Ferroelectric properties

Figure 4 shows a typical polarization–electric field (*P*-*E*) hysteresis loop for the BZT films on Pt/Ti/SiO_2/Si, LSMO/Pt/Ti/SiO_2/Si, and LSMO/Si substrates annealed at 650 °C for 10 min in oxygen atmosphere. The remanent polarization (P_r) and the coercive electric field (E_c) obtained from the *P*-*E* hysteresis loops are 0.937 $\mu C/cm^2$ and 9.4 kV/cm, 0.471 $\mu C/cm^2$ and 7.69 kV/cm, and 4.43×10^{-3} $\mu C/cm^2$ and 6.38 kV/cm, respectively, for BZT films on Pt/Ti/SiO_2/Si, LSMO/Pt/Ti/SiO_2/Si, and LSMO/Si substrates. The P_r value of the BZT film on LSMO/Si substrate is much smaller than those of BZT films on Pt/Ti/SiO_2/Si and LSMO/Pt/Ti/SiO_2/Si substrates. The P_r and E_c values both are smaller than that of BZT(15/85) film (P_r=3.31 $\mu C/cm^2$, E_c=93.5 kV/cm).[7] Use of the conductive oxide electrode LSMO did not enhance the ferroelectric properties of the BZT films.

C. Dielectric properties and tunability

The dc bias field dependence of dielectric constant and dielectric loss at room temperature (25 °C) was measured to evaluate the tunability of the BZT/LSMO heterostructure thin film. The measurements were conducted by applying a small ac signal of 0.5 V amplitude and 1 MHz frequency while the dc field was swept from positive bias to negative bias. The potential of the BZT films to be used in voltage-

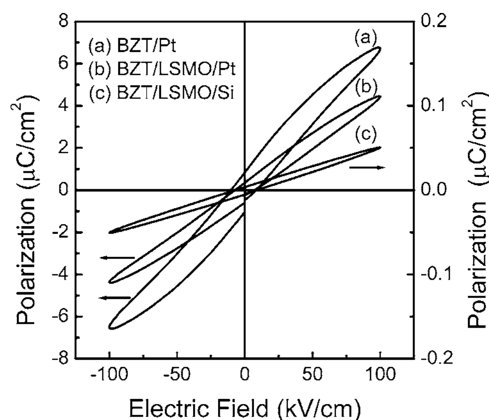

FIG. 4. Polarization vs electric field hysteresis loops of the BZT thin films deposited on (a) Pt/Ti/SiO_2/Si, (b) LSMO/Pt/Ti/SiO_2/Si, and (c) LSMO/Si substrates and crystallized *in situ* at 650 °C for 10 min.

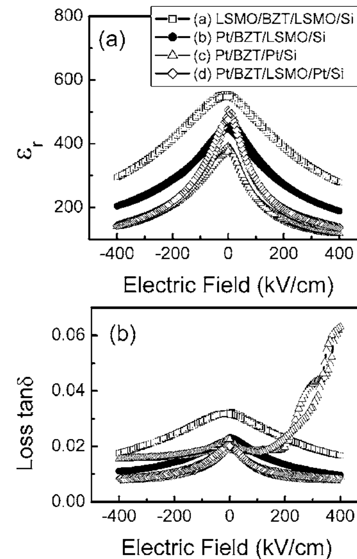

FIG. 5. Electric field dependence of the (a) dielectric constant ε_r and (b) loss tan δ of the four types of BZT thin film capacitors.

tunable devices depends on the ability to change the dielectric constant by means of an applied electric field. The electric field dependence of the dielectric constant (ε_r) and loss tan δ at room temperature is shown in Fig. 5. As expected, a slim hysteresis was observed in these characteristics, as a result of the existence of ferroelectric domains at room temperature. The dielectric constant and dissipation factor are 555 and 0.032, 476 and 0.023, 392 and 0.019, and 506 and 0.019, respectively, for the LSMO/BZT/LSMO/Si, Pt/BZT/LSMO/Si, Pt/BZT/Pt/Si, and Pt/BZT/LSMO/Pt/Si capacitors at 1 MHz and zero field. A dielectric constant (ε) of 121 was reported for sol-gel derived BZT(5/95) films.[10] A series of ε values of 100, 150, and 250 has been reported for BZT(20/80) films on Pt-coated Si substrates with various deposition temperatures prepared by sputtering.[8] An ε value of 452 has been reported for BZT(10/90) thin film on Pt-coated Si substrate prepared by the PLD technique.[20] The LSMO bottom layer enhanced the dielectric properties. From Figs. 5(c) and 5(d), it can be seen that the dielectric loss of BZT improved for the LSMO buffer layer electrode versus the non-buffer-layer electrode stack. It is well known that conducting oxide electrodes, such as LSMO, aid in mitigation of oxygen vacancy, hence this is a possible reason for the improvement in the dielectric loss of the BZT/LSMO/Pt film.

The tunability is defined as $[\varepsilon_r(0)-\varepsilon_r(E)]/\varepsilon_r(0)$, where $\varepsilon_r(0)$ and $\varepsilon_r(E)$ are the dielectric constants measured at zero and a non-zero E field, respectively. The figure of merit (FOM) is defined as the tunability/loss. The dielectric constant, loss, tunabilities, and FOMs are shown in Fig. 5 and Table II. From Fig. 5 and Table II, these tunabilities and FOMs are 49.9% and 15.6, 60.3% and 26.2, 69.9% and 36.8, and 72.9% and 38.4, respectively, for the LSMO/BZT/LSMO/Si, Pt/BZT/LSMO/Si, Pt/BZT/Pt/Si, and Pt/BZT/LSMO/Pt/Si capacitors. The tunability and FOM of the Pt/BZT/LSMO/Si capacitor are higher than those of the LSMO/BZT/LSMO/Si capacitor, but the latter has higher dielectric constant. Similarly, the tunability and FOM of the

TABLE II. The dielectric constant ε_r, loss tan δ, tunability, and FOM for the various capacitors at 1 MHz and E=400 kV/cm.

Capacitors	$\varepsilon_r(0)$	tan δ	$\varepsilon_r(E)$	Tunability (%)	FOM
LSMO/BZT/LSMO/Si	555	0.032	278	49.9	15.6
Pt/BZT/LSMO/Si	476	0.023	189	60.3	26.2
Pt/BZT/Pt/Ti/SiO_2/Si	392	0.019	118	69.9	36.8
Pt/BZT/LSMO/Pt/Ti/SiO_2/Si	506	0.019	137	72.9	38.4

Pt/BZT/LSMO/Pt/Si capacitor are higher than those of the Pt/BZT/Pt/Si capacitor.The values are higher than those of pulsed laser deposited random-oriented BZT(15/85) films (45% at 200 kV/cm),[7] and higher than those of sol-gel derived BZT(35/65) films (38% at 600 kV/cm).[15] Padmini *et al.*[21] reported that when a BST film was subjected to tensile stress, a contraction occurred along the *c* axis leading to an enhancement of the in-plane oriented polar axis. By a converse electrostrictive effect, the in-plane tensile stress reduces the capacitance in the thickness direction of the film.[22] When higher voltages or electric fields were applied to the (100)-oriented BST thin films, the in-plane orientation of the polar axis resulted in higher tunability. Hence, the tunability of (100)-oriented BZT films was also of a high value. On the other hand, interfaces between the ferroelectric thin films and the electrodes affect the measured dielectric properties.

D. Influence of the interfacial layer on the dielectric properties

It has been proposed that the reduction of ε_r in ferroelectric thin films can be explained by the existence of an interfacial "dead layer" at one or both metal electrodes with poor dielectric properties.[2,23,24] This may arise from the oxygen interdiffusion, chemical reaction, structural defects, or Schottky barriers at the interfaces. The relationship of the Pt/BZT/Pt capacitances of each capacitor can be expressed as

$$\frac{1}{C}=\frac{1}{C_b}+\frac{1}{C_i}, \tag{1}$$

where C is the measured capacitance, C_b is the bulk film capacitance, and C_i is the capacitance of the interfacial dead layer. Therefore, the measured dielectric constant (ε_r) is

$$\frac{d}{\varepsilon_r}=\frac{d_b-d_i}{\varepsilon_b}+\frac{d_i}{\varepsilon_i}. \tag{2}$$

If $d_b \gg d_i$, then

$$\frac{d}{\varepsilon_r}=\frac{d_b}{\varepsilon_b}+\frac{d_i}{\varepsilon_i}=\frac{d}{\varepsilon_b}+d_i\left(\frac{1}{\varepsilon_i}-\frac{1}{\varepsilon_b}\right), \tag{3}$$

where d, d_b, and d_i are the thickness of the measured film, the thickness of the BZT bulk film layer, and the thickness of the nonbulklike interfacial layer. ε_b and ε_i are the dielectric constant of the BZT bulk film and the dielectric constant of the nonbulklike interfacial layer. These equations have been widely used to model thickness-dependent dielectric properties.[23–27] From Eq. (2), the ε_r decreased with the decrease of ε_i value. Experimental verification has been done by Lee and Hwang[25] and Parker *et al.*[26] in the Pt/BST/Pt system, the decrease of ε_r with decreasing thickness of the BST thin films is due to the existence of an interfacial dead layer in the Pt/BST interfacial surface.

However, for the Pt/BZT/LSMO capacitor, the influence of the two interfaces of Pt/BZT and BZT/LSMO on the dielectric properties is actually quite different. As discussed by Vendik *et al.*,[28] the polarization of a dielectric layer can penetrate into the oxide electrodes, meaning that the dielectric/oxide interface can be characterized by free-boundary conditions. In other words, the influence of the ferroelectric/oxide interface can be eliminated and there would be no significant thickness dependence in an oxide/BST/oxide heterostructure. These assertions have been experimentally verified by Hwang *et al.*[29,30] and Dittmann *et al.*[31] in the IrO_2/BST/IrO_2 and $SrRuO_3$/BST/$SrRuO_3$ structures. The decrease in the measured dielectric constant of BST thin films having Pt electrodes with decreasing dielectric film thickness was attributed to the finite charge-screening length of the metal electrode and the intrinsic dead layer of the dielectric surface. On the other hand, the almost film-thickness-independent dielectric constant of the BST thin films with conducting oxide electrodes, IrO_2 and $SrRuO_3$, was attributed to the very high capacitance values of the charge-screening layer of the oxide electrodes. The very high capacitance value appeared to originate from the strain-induced high dielectric constant of the oxide electrodes.[30] Use of the conductive oxide electrodes, such as LSMO, $CaRuO_3$, $LaNiO_3$, and YBCO, can decrease the thickness of the dead layer[30–33] and enhance the dielectric constant and tunability,[2,11–14,30–33] so that the Pt/BZT/LSMO capacitor has higher dielectric constant and tunability, and the LSMO/BZT/LSMO/Si capacitor have the highest dielectric constant. The very high capacitance value appeared to originate from the strain-induced high dielectric constant of the oxide electrodes.[30]

IV. CONCLUSIONS

In conclusion, the high (100)-oriented BZT thin films were deposited on LSMO/Si and LSMO/Pt/Ti/SiO_2/Si substrates by a pulsed laser deposition method. For four capacitors of LSMO/BZT/LSMO/Si, Pt/BZT/LSMO/Si, Pt/BZT/Pt/Si, and Pt/BZT/LSMO/Pt/Si, the dielectric and ferroelectric properties are measured. The LSMO/BZT/LSMO/Si and Pt/BZT/Pt/Si capacitors have the highest dielectric constant and the highest remanent polarization, respectively. The dependence of dielectric constant and tunability of the films on the electric field was investigated and the Pt/BZT/LSMO/Pt/Si capacitors have the highest tunability and figure of merit. Using conductive oxide LSMO

electrode enhanced the dielectric properties of BZT films. The LSMO/BZT/LSMO capacitor has the highest dielectric constant. The high dielectric constant have been attributed to the (100) texture of the LSMO bottom layer leading to decrease of the thickness of the dead layer and attributed to the strain-induced high dielectric constant of the oxide electrodes. The BZT thin film is an attractive candidate for microwave tunable device applications.

ACKNOWLEDGMENTS

This work is supported by the Guangdong Provincial Natural Science Foundation of China (Grant Nos. 04300168 and 05001825), the Postdoctoral Fellowship Scheme, and the Centre for Smart Materials of the Hong Kong Polytechnic University.

[1]M. W. Cole, W. D. Nothwang, C. Hubbard, E. Ngo, and M. Ervin, J. Appl. Phys. **93**, 9218 (2003).
[2]X. X. Xi, H. C. Li, W. D. Si, A. A. Sirenko, I. A. Akimov, J. R. Fox, A. M. Clark, and J. H. Hao, J. Electroceram. **4**, 390 (2000).
[3]D. Hennings, A. Schnell, and G. Simon, J. Am. Ceram. Soc. **65**, 539 (1982).
[4]U. Weber, G. Greuel, U. Boettger, S. Weber, D. Hennings, and R. Waser, J. Am. Ceram. Soc. **84**, 759 (2001).
[5]Z. Yu, C. Ang, R. Guo, and A. S. Bhalla, Appl. Phys. Lett. **81**, 1285 (2002).
[6]X. G. Tang, K. H. Chew, and H. L. W. Chan, Acta Mater. **52**, 5177 (2004).
[7]A. R. James and C. Prakash, Appl. Phys. Lett. **84**, 1165 (2004).
[8]W. S. Choi, B. S. Jang, D. G. Lim, J. Yi, and B. Hong, J. Cryst. Growth **237–239**, 438 (2002).
[9]A. Dixit, S. B. Majumder, R. S. Katiyar, and A. S. Bhalla, Appl. Phys. Lett. **82**, 2679 (2003).
[10]X. G. Tang, H. L. W. Chan, and A. L. Ding, Thin Solid Films **460**, 227 (2004).
[11]S. G. Lu, X. H. Zhu, C. L. Mak, K. H. Wong, H. L. W. Chan, and C. L. Choy, Appl. Phys. Lett. **82**, 2877 (2003).
[12]Y. A. Jeou, E. S. Choi, T. S. Seo, and S. G. Yoon, Appl. Phys. Lett. **79**, 1012 (2001).
[13]K. H. Yoon, J. H. Sohn, and B. D. Lee, Appl. Phys. Lett. **81**, 5012 (2002).
[14]D. Galt, J. C. Price, J. A. Beall, and R. H. Ono, Appl. Phys. Lett. **63**, 3078 (1993).
[15]J. Zhai, X. Yao, L. Zhang, and B. Shen, Appl. Phys. Lett. **84**, 3136 (2004).
[16]X. G. Tang, J. Wang, X. X. Wang, and H. L. W. Chan, Solid State Commun. **131**, 163 (2004).
[17]R. K. Zheng, C. F. Zhu, J. Q. Xie, R. X. Huang, and X. G. Li, Mater. Chem. Phys. **75**, 121 (2002).
[18]X. Tang, J. Wang, and H. L. W. Chan, J. Cryst. Growth **276**, 453 (2005).
[19]X. G. Tang, J. Wang, Y. W. Zhang, H. L. W. Chan, A. L. Ding, and C. L. Choy, Appl. Phys. A: Mater. Sci. Process. **78**, 1205 (2004).
[20]S. Halder, S. Bhattacharyya, and S. B. Krupanidhi, Mater. Sci. Eng., B **95**, 124 (2002).
[21]P. Padmini, T. R. Taylor, M. J. Lefevre, A. S. Nagra, R. A. York, and J. S. Speck, Appl. Phys. Lett. **75**, 3186 (1999).
[22]T. M. Shaw, Z. Suo, M. Huang, E. Liniger, R. B. Laibowitz, and J. D. Baniecki, Appl. Phys. Lett. **75**, 2129 (1999).
[23]C. Zhou and D. M. Newns, J. Appl. Phys. **82**, 3081 (1997).
[24]C. Basceri, S. K. Streiffer, A. I. Kingon, and R. Waser, J. Appl. Phys. **82**, 2497 (1997).
[25]B. T. Lee and C. S. Hwang, Appl. Phys. Lett. **77**, 124 (2000).
[26]C. B. Parker, J. P. Maria, and A. I. Kingon, Appl. Phys. Lett. **81**, 340 (2002).
[27]U. Ellerkmann, R. Liedtke, U. Boettger, and R. Waser, Appl. Phys. Lett. **85**, 4708 (2004).
[28]O. G. Vendik, S. P. Zubko, and L. T. Ter-Martirosayn, Appl. Phys. Lett. **73**, 37 (1998).
[29]C. S. Hwang *et al.*, J. Appl. Phys. **85**, 287 (1999).
[30]C. S. Hwang, J. Appl. Phys. **92**, 432 (2002).
[31]R. Dittmann, R. Plonka, E. Vasco, N. A. Pertsev, J. Q. He, C. L. Jia, S. Hoffmann-Eifert, and R. Waser, Appl. Phys. Lett. **83**, 5011 (2003).
[32]B. Chen, H. Yang, J. Miao, L. Zhao, L. X. Cao, B. Xu, X. G. Qiu, and B. R. Zhao, J. Appl. Phys. **97**, 024106 (2005).
[33]T. M. Shaw, S. Trolier-McKinstry, and P. C. McIntyre, Annu. Rev. Mater. Sci. **30**, 263 (2000).

Journal of Applied Physics is copyrighted by the American Institute of Physics (AIP). Redistribution of journal material is subject to the AIP online journal license and/or AIP copyright. For more information, see http://ojps.aip.org/japo/japcr/jsp